Stress distribution changes in bovine vertebrae just below the endplate after creep loading

van Dieen, J.H.; Kingma, I.; Meijer, R.; Hansel, L.; Huiskes, R.

published in
Clinical Biomechanics
2001

DOI (link to publisher)
10.1016/S0268-0033(00)00105-4

ELSEVIER

Clinical Biomechanics 16 Supplement No. 1 (2001) S135–S142

CLINICAL BIOMECHANICS

www.elsevier.com/locate/clinbiomech

Stress distribution changes in bovine vertebrae just below the endplate after sustained loading

Jaap H. van Dieën [a,*], Idsart Kingma [a], Riske Meijer [a], Layla Hänsel [a], Rik Huiskes [b]

[a] *Amsterdam Spine Unit, Institute for Fundamental and Clinical Human Movement Sciences, Vrije Universiteit Amsterdam, Amsterdam NL-1081 BT, Netherlands*

[b] *Biomechanics laboratory, Department of Orthopaedics, Institute for Fundamental and Clinical Human Movement Sciences, University of Nijmegen, Nijmegen, Netherlands*

Abstract

Objective. To describe the pattern of stress distribution in the vertebral body just behind the endplate, and to document its changes due to sustained loading.

Methods. Twelve fresh bovine coccygeal motion segments were dissected and tested. Each specimen was axially loaded with a sustained compressive force of 50% of its estimated compressive strength. Before loading, after 1.5 h and after 3 h of loading, the distribution of the axial pressure under the bottom vertebra (i.e., just below its top endplate) was recorded at three force levels (25%, 37.5% and 50% of the estimated compressive strength), using pressure-sensitive film.

Results. Stress distribution over the endplate was found to be fairly uniform. At low compression forces, the stress was the highest centrally. With increased compression and after sustained compression the uniformity improved through a significant redistribution of stress to the periphery. No stress peaks were found to occur after sustained loading.

Conclusion. Stress peaks after sustained loading cannot explain the occurrence of endplate fractures in sustained cyclic compression in non-degenerated discs. Competing explanations, such as creep, and fatigue failure, would appear more likely candidates.

Relevance

It has been hypothesised that compression induced fractures of the lumbar vertebral endplate constitute an important etiological factor for low back pain. Competing theories exist on the fracture mechanism in sustained loading and these would have different implications with respect to prevention. The present study evaluated one of these theories.

Keywords: Spine; Intervertebral disc; Compression; Endplate fractures

1. Introduction

It has been hypothesised that compression-induced fractures of the lumbar vertebral endplate and the underlying trabecular bone constitute an important etiological factor for low back pain [1]. The strength of human lumbar vertebrae in compression is determined mainly by the product of their cross-sectional area and bone density and ranges from about 2–10 kN [2,3]. Comparison of these in vitro strength values with estimates of compression forces working on the spine in vivo during physically exerting tasks such as lifting suggests that compression fractures are quite likely to occur [4]. This is even more likely in repetitive loading, as it has been shown that spinal motion segments fail at much reduced forces in this case [5,6]. The assumption that compression fractures occur rather frequently is supported by post-mortem evidence of healed fractures of the endplate and underlying trabecular bone in a large fraction of samples studied [7–11]. It is as yet unclear what the mechanism behind the occurrence of damage in cyclic loading exactly is. Failure in 1 Hz cyclic loading has been predicted equally well with creep failure and fatigue failure models [4]. In addition, it has been shown that fluid loss from the centre of the intervertebral disc due to sustained or repeated loading changes the stress pattern within the disc [12]. With fluid loss, the pressure in the nucleus pulposus was found to decrease, whereas the pressure in the anulus fibrosus increased. In some specimens after sustained loading,

* Corresponding author.
E-mail address: j_h_van_dieen@fbw.vu.nl (J.H. van Dieën).

0268-0033/01/$ - see front matter
PII: S0268-0033(00)00105-4

high peaks in the pressure profile were found within the anulus [13]. The changed disc pressure profile is likely to be reflected in the pattern of stress distribution over the vertebral endplate and, consequently, in the underlying vertebral body. This may affect the probability of failure in repeated loading, since local stress peaks induced by fluid redistribution might exceed tissue tolerance.

To date, the stress distribution over the vertebral endplate has hardly been studied. Horst and Brinckmann [14] used piezo-electric pressure transducers to measure the stress component perpendicular to the endplate at five locations, one underlying the central nucleus and four located either at the border between nucleus and anulus or in the middle of the anulus depending on the specimen. They showed a uniform distribution of stress over these locations in both non-degenerated and degenerated discs under axial loading at low forces (<1000 N). Under eccentric loading the stress in the anulus increased in the degenerated specimens. Ranu et al. [15,16] tested specimens at higher compression forces after placing pressure transducers within 10 mm from the anterior and lateral edges of the vertebra. They report linear relations between compression force and pressure with marked inhomogeneities of the distribution. The effect of sustained or repeated loading on the stress distribution over the endplate has been studied even less. One study showed a relaxation of the pressure under the nucleus but no changes of the vertical stress under the anulus [17]. Responses were investigated up to 100 s only.

The current study was undertaken to describe the pattern of stress distribution in the vertebral body just behind the endplate, and to document its changes due to sustained submaximal loading. It was hypothesised that with sustained loading the vertical stress on the central endplate would decrease reflecting, the loss of pressure in the nucleus. Correspondingly the stress on the peripheral endplate was expected to increase and the occurrence of stress peaks in the periphery of the endplate was anticipated.

2. Methods

Twelve fresh bovine coccygeal motion segments (consisting of one intervertebral disc and the two adjacent vertebrae) were dissected and tested within 72 h. Specimens were stored wrapped in cling film at 5°C. The outer vertebral endplates were embedded in Poly-MethylMethAcrylate (PMMA) using a circular mould of 5 cm diameter. The following procedure was applied to ensure that only pure axial forces were applied, to avoid failure of the specimen in shear during the test. The PMMA layers were clamped into 6 cm diameter fixtures using screws (Fig. 1). Subsequently, they were dynamically loaded at 10–300 N in a materials testing machine

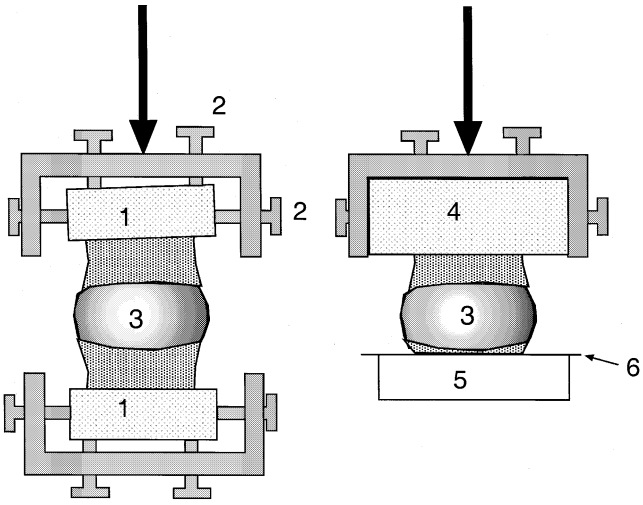

Fig. 1. Schematic illustration of the set-up used to ensure pure axial loading and the measurement set-up (left) and to perform the measurements (right). 1 = 5 cm PMMA; 2 = screws; 3 = specimen; 4 = 6 cm PMMA; 5 = glass plate; 6 = pressure-sensitive film.

(MTS, DSTS 3301). The lower fixture was equipped with strain gauges to measure both compression and shear components of the force transmitted through the bottom vertebra. This was used to align the specimen by means of the screws in the fixtures, such that only a pure compression load component remained. Subsequently the specimens were again embedded in PMMA using the fixtures as moulds. In this way loading perpendicular to the surface of the final PMMA layers was guaranteed to be purely axial. The PMMA layer at the bottom vertebra was used to guide cutting the bottom vertebra parallel to the surface of this layer (i.e., perpendicular to the loading direction) just below its top endplate. Subsequently, the cut surface was slightly polished.

Ultimate compressive strength (UCS) of each specimen was estimated on the basis of the relationship found in pilot data between strength of bovine coccygeal motion segments and their cross-sectional areas. Each specimen was axially loaded with a sustained compressive force of 50% UCS. Before loading, after 1.5 and 3 h of loading, the loading was interrupted to record the distribution of the axial pressure under the bottom vertebra (i.e., just below its top endplate) at three force levels (25%, 37.5% and 50% UCS). The order of the three measurements was randomised over specimens, but constant within specimens. The experimental protocol is illustrated in Fig. 2.

Measurements were performed using pressure-sensitive film (Fuji, multipurpose pressure measurement film, low pressure 2.5–10 MPa). The films were scanned (Starscan 4800; 600 DPI, 256 grey values) for further analysis. It was preferred not to calculate stress values from the grey values, in the view of non-linear relationship between stress and colour intensity [18]. All

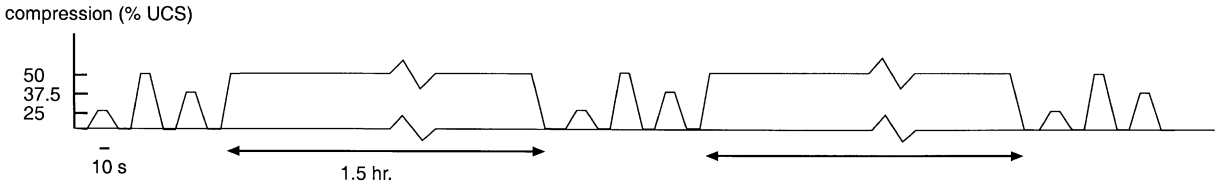

Fig. 2. Example of the time series of the compression force applied to the specimens.

grey values were normalised to the maximum colour intensity documented across all images. To analyse the same area in all scans, the images of one specimen were rotated and translated using standard graphical software such that orientations and positions of the centre of the image were identical. The area circumscribing the largest image of each specimen (typically acquired at 50% UCS after 3 h) was defined as the area of interest. Only the data for pixels within this area were taken into account. The number of pixels in the scan which were coloured (stress above threshold of the film, specified at 2.5 MPa) was used as an indicator of the area the stress was distributed over. The cumulative probability distribution function of all grey values in each scan was calculated and the 5th, 50th and 95th percentiles intensities were determined as indicators of minimum, median and peak stress respectively. The same figures (5th, 50th and 95th percentile intensities) were derived for the centre and the outer one-fourth of the surface of the area of interest. Finally the product of the mean grey value and the number of pixels above the sensitivity threshold was calculated and correlated to the compression force applied, to check the validity of the method.

A repeated measures ANOVA was used to test for effects of force and time on the dependent variables. When the sphericity assumption was violated, Wilk's Lambda was used for testing, in all other cases the F-statistic was used.

3. Results

Fig. 3 presents a typical example of the images obtained and Fig. 4 gives the corresponding frequency distribution of grey values. As can be seen with compression force and time the coloured area increases and the number of pixels with minimal grey values diminishes, indicating an increase of the area over which the pressure is distributed. Overall, the distributions of grey values are fairly uniform with many pixels in the same or neighbouring bins of the histogram. As can be seen from the histograms neither force nor time has a dominant effect on the peak grey values.

The increase in the area over which the stress was distributed with increasing compression force, represented by the number of pixels above the sensitivity threshold appeared to be significant ($P < 0.001$; Fig. 5(a)). In addition the median stress depended on the compression force applied, since the median grey value was affected by compression ($P < 0.001$; Fig. 5(b)), though no significant difference was found between 37.5% UCS and 50% UCS. A qualitatively similar but much less strong effect of compression force was found on the 95th percentile grey value ($P = 0.012$; Fig. 5(c)). The 5th percentile grey value clearly increased with each step in compression force ($P < 0.001$; Fig. 5(d)). The changes in compression force were accompanied by a slight increase in central stress and a strong increase in the peripheral stress, as indicated by significant increases of the median grey values in the inner one fourth of the image ($P = 0.003$; Fig. 6(a)) and in the outer one fourth ($P < 0.001$; Fig. 6(b)).

Sustained compression caused an increase of the area over which the stress was distributed, as was indicated by an increase of the number of pixels above the sensitivity threshold ($P = 0.007$; Fig. 5(a)). The median grey value, indicative of the median stress, was not significantly affected by sustained compression ($P = 0.063$; Fig. 5(b)). Peak stress was slightly reduced by sustained compression, as indicated by a significant time effect on the 95th percentile grey value ($P = 0.002$; Fig. 5(c)). A significant interaction effect of time and compression force on the 5th percentile grey value was found ($P < 0.001$; Fig. 5(d)). At 25% UCS no change was found, whereas at the higher compression forces the 5th percentile grey value increased between the pre-load measurements and the measurements after 1.5 h. The reduction in the 95th percentile and more importantly the increase in the 5th percentile grey values indicate an increased uniformity of the stress distribution. This was further corroborated by a reduction of the median grey value in centre one fourth of the image ($P = 0.025$; Fig. 6(a)) and a concomitant increase of the median grey value in the outer one fourth of the image ($P = 0.046$; Fig. 6(b)).

The grey values cannot be directly translated into stress values, since the coefficients of correlation between the product of the surface integrated grey value and the compression forces applied to the specimens are overall only moderate (Table 1). Within specimens the correlations, were much stronger with a median coefficient of 0.96.

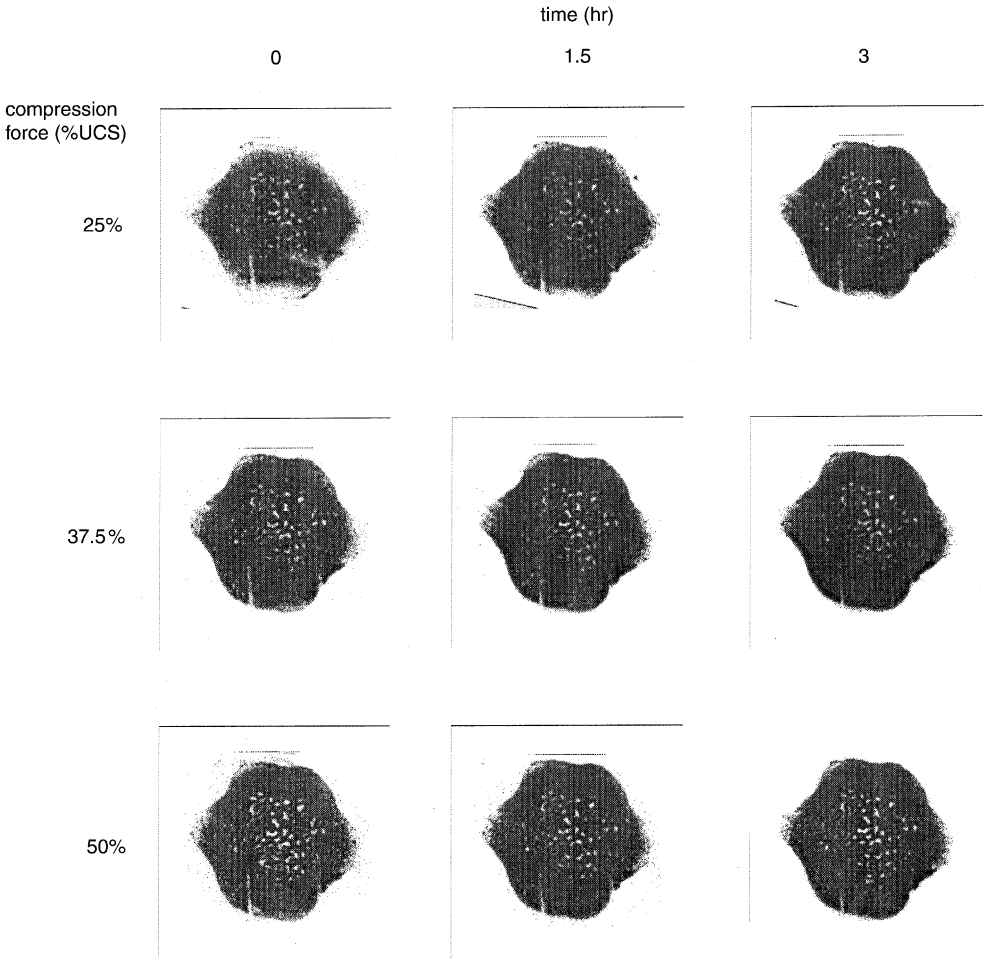

Fig. 3. Typical example of the images obtained after scanning the pressure films. The columns indicate the levels of compression force (25%, 37.5% and 50% UCS respectively), the rows indicate the levels of time during which sustained compression had been applied (0, 1.5 and 3 h, respectively).

4. Discussion

The distribution of stress over the endplates of bovine coccygeal motion segments in the longitudinal direction was inferred from the colour intensity of pressure-sensitive films placed just beneath the endplate of the transversely sectioned lower vertebra, while applying axial compression at the intact top vertebra. The stress distribution appeared to be fairly uniform. With increased compression force up to 50% of the estimated maximum compression force, the area over which the stress was distributed increased and consequently the stress distribution became even more uniform, resulting in only minor effects of compression force on peak stress. After sustained compression, the stress in the central part of the endplate slightly decreased, whereas it increased in the periphery. This also resulted in an increased uniformity of the stress distribution and stress peaks were not found to develop. In contrast, peak stress slightly decreased with time.

We chose to perform this experiment using bovine coccygeal motion segments for their easy availability and because this offered the possibility to test the material without it having been frozen, since freezing has been shown to affect creep properties of the intervertebral disc [19]. The main differences with human lumbar segments are the lower cross-sectional area, higher apparent bone density, and the endplate convexity toward the disc. Nevertheless, in our view these motion segments provide a satisfactory model for the mechanics of the human lumbar spine in qualitative studies such as the present one. Human lumbar discs and bovine tail discs have been demonstrated to be biochemically similar [20]. In addition, water content has been shown to be comparable [12,21]. These similarities result in similar time constants of creep deformation when under compression. The average time constant for four bovine coccygeal motion segments was: 2687 s [22]. For human lumbar and thoracic specimens a range of 1351–61728 s with a mean value of 6667 s has been reported [23]. Finally, unpublished data collected in preparation of this experiment suggest that trabecular orientation, distribution of trabecular density and strength are also highly comparable to human segments.

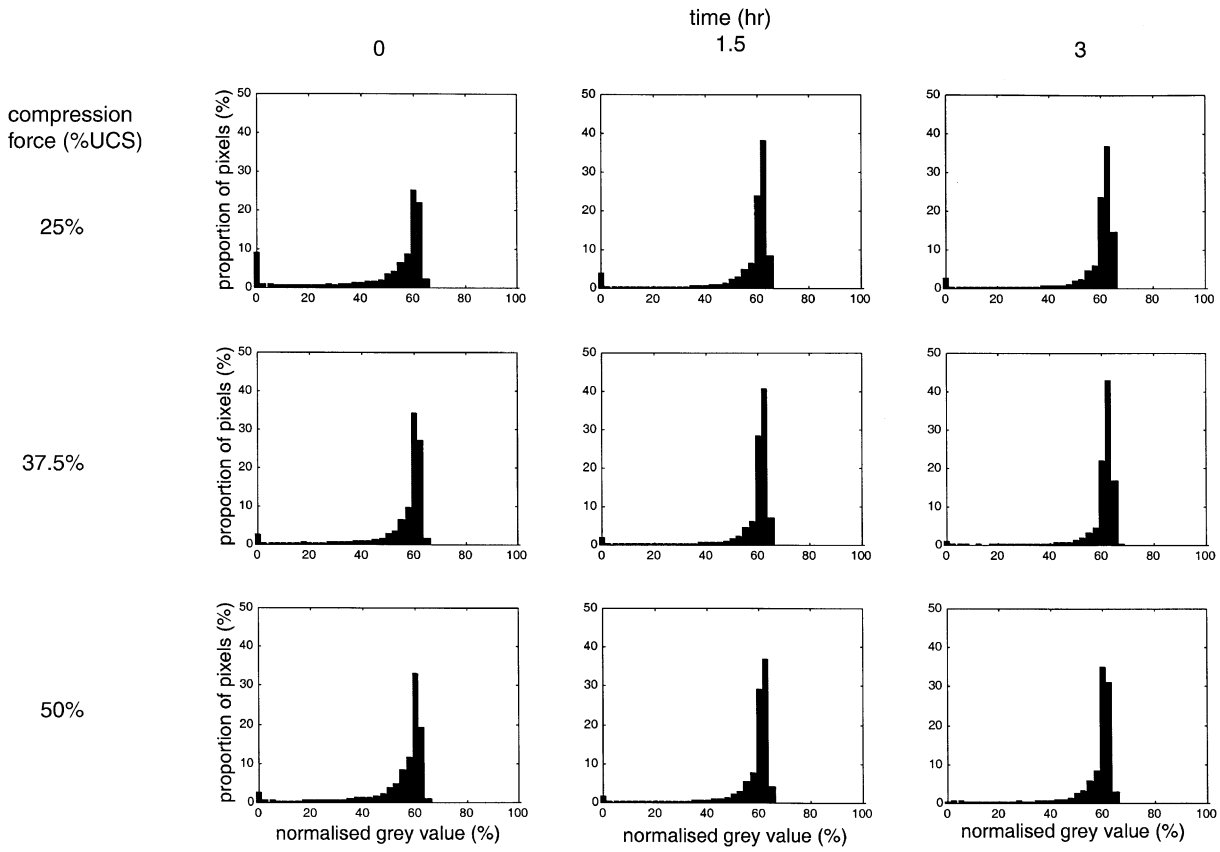

Fig. 4. Typical example of the distribution of the normalised grey values of the scanned pressure films (same data as in Fig. 3). The columns indicate the levels of compression force (25%, 37.5% and 50% UCS respectively), the rows indicate the levels of time during which sustained compression had been applied (0, 1.5 and 3 h, respectively).

The compression force applied in this study (50% UCS) over a 3 h period is certainly rather high. In vivo compressional loading in humans during physically exerting tasks will exceed 50% UCS, but is generally dynamic in nature. Sustained loading at this level is not likely to occur. We choose to use this high level, since this being the first study addressing the effects of sustained loading on the stress distribution over the endplate, we wanted to increase the probability of causing stress peaks. We therefore believe that at more physiological load levels stress peaks are even more unlikely to occur. In addition the loading applied was pure axial compression. In vivo high compression forces will be combined with shear forces and probably deformation (bending or torsion) of the disc. This combined loading may in itself cause stress peaks on the endplate and it is unsure how these peaks would be affected by sustained loading.

To what extent the sawing and polishing of the specimens has affected the results cannot be ascertained. It is possible that the presence of a stiff cortical shell as a supporting structure in the periphery would increase the stress in peripheral endplate. However, previous model studies have indicated that the cortical shell plays a limited role in sustaining compression forces especially near the endplates [24].

The use of pressure film to measure the stress distribution has several obvious limitations. The sensitivity range of the film (2.5–10 MPa) does not allow complete mapping of the distribution. With respect to the aim of the study, the upper threshold is the most troublesome. Due to this upper limit, peak stress might go undetected. The data however suggest that this does not play an important role. When normalised to the maximum grey value documented, a large majority of all grey values was well below 100% (Fig. 4). In addition, the distributions of the grey values as shown in the example of Fig. 2 are not suggestive of saturation effects. This suggests that the main conclusions with respect to the effects of sustained compression are valid. Finally, there was a moderate correlation between the compression force applied and the product of the number of pixels above sensitivity threshold and the mean grey value. The coefficients of correlation were highest for the highest compression forces and higher after 3 h than pre-loading, indicating that the lower threshold did disturb the relationship between surface integrated grey value and compression much more than the upper threshold of

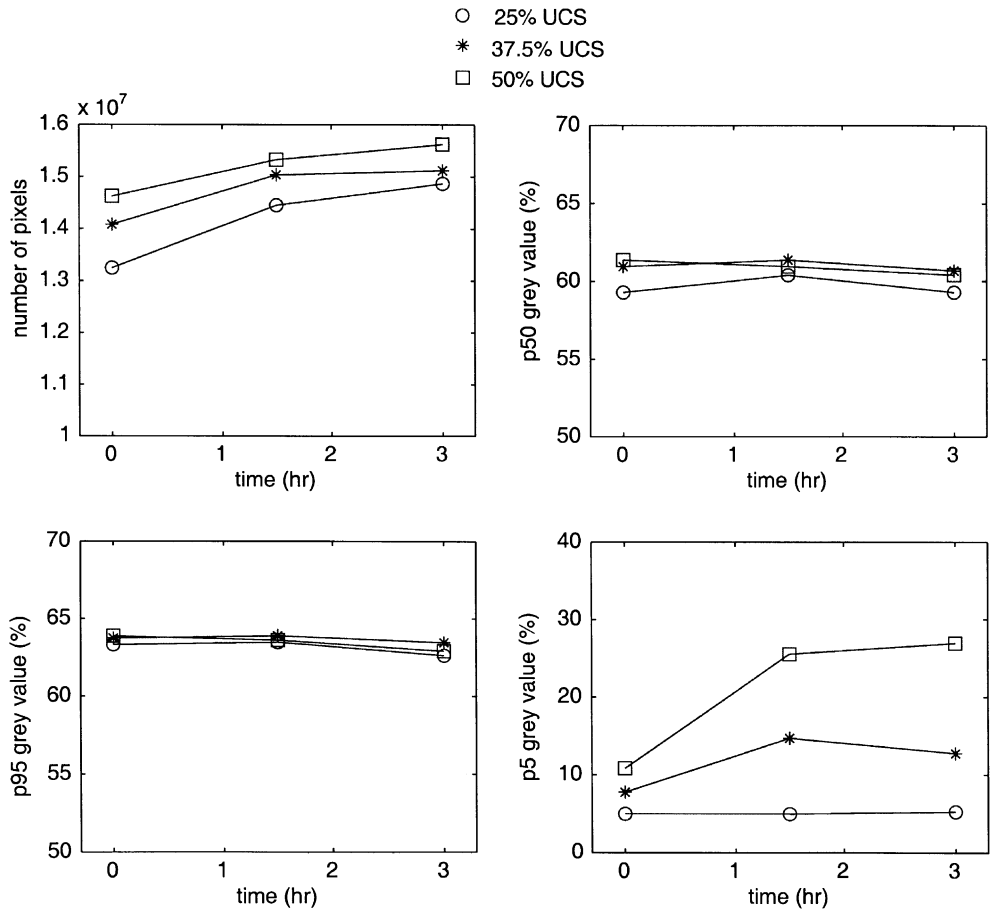

Fig. 5. Effects of time (horizontal axis) and force (separate lines) on the number of pixels above sensitivity threshold (a) and on the median (b), 95th percentile (c), and 5th percentile (d) normalised grey values of the complete image.

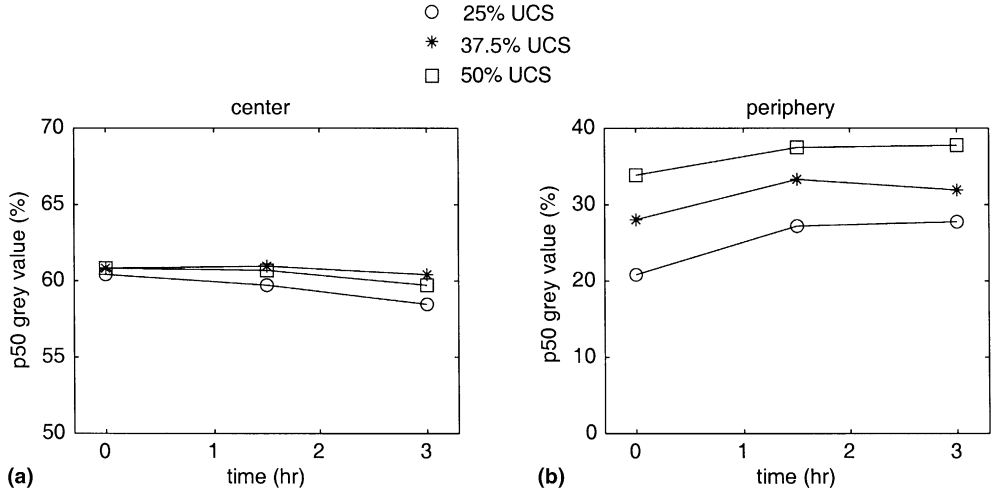

Fig. 6. Effects of time (horizontal axis) and force (separate lines) on the median normalised grey values in the inner (a) and outer (b) one-fourth of the scanned image.

sensitivity. The lower threshold implies that the increase in area above threshold is an overestimation of the increase in area carrying compression. The initial distribution of the vertical stress appeared fairly uniform with the exclusion of the outer rim of the endplate and vertebra. This finding corresponds with the data

Table 1
Coefficients of correlation ($n = 12$) between surface integrated grey values and compression forces applied

Time	Compression force		
	25% UCS	37.5% UCS	50% UCS
0 h	0.23	0.38	0.58
1.5 h	0.62	0.74	0.82
3 h	0.68	0.78	0.86

provided by Horst and Brinckmann [14], but contrasts with the data presented by Ranu et al. [15]. The latter may be due to the placement of the transducers in the study by Ranu et al. which was close to the outer rim of the vertebra. The lower axial stress on the outer rim of the endplate is probably explained by tensile forces exerted on the endplate by fibres of the anulus fibrosus.

With sustained loading, a redistribution of axial stress from inner to the outer area of the vertebra occurred. This corresponds well with the finding that pressure in the intervertebral disc is redistributed from the inner to the outer region [12,13]. This redistribution of pressure in the disc is caused by a loss of water from the disc, with the highest decrease in water content in the central part of the disc [12,22]. In addition, relaxation of anulus fibres might contribute to this redistribution, Whereas intra-discal pressure has been found to be less uniform after sustained loading [12,13], the endplate stress was still and even slightly more uniformly distributed after sustained loading. There may be several explanations for this disparity. One explanation might be that peaks in fluid pressure in the intervertebral disc are partially offset by increased tension in nearby anulus fibres, which could eliminate stress peaks at the level of the endplate. Another explanation might be that the pressure peaks measured in the disc were caused by contacts of the pressure transducer with solid materials [25]. Finally, the effects of sustained loading may depend on the condition of the disc, with more peaks occurring in more degenerated specimens. The bovine specimens tested here, in contrast to human specimens tested in previous studies, showed no signs of degeneration. Thus the implications of this study are limited to non-degenerated spines.

The bulge of the endplate into the vertebral body was found to increase over time during cyclic loading of human specimens [26]. This could indicate an increasing instead of decreasing axial stress in the centre of the vertebral body, which would contrast with our findings. However, an alternative explanation, could be a decrease of the load bearing capacity of the endplate and trabecular support over time. Such a decrease, most likely due to creep or fatigue failure, seems the most plausible explanation for these seemingly contrasting results. In addition, morphological differences between human lumbar motion segments and bovine coccygeal specimens, in particular the difference in endplate curvature (convex towards the disc in bovine specimens) may play a role.

The fluid loss due to sustained or repeated compression can be likened to the changes taking place over a longer time scale in the ageing or degenerating disc. Finite element model studies employing time-independent material properties have predicted a similar shift of the stress from the centre to the periphery of the endplate and in the underlying vertebral body in degenerated specimens [24,27,28]. These findings appear to be in contrast with the absence of an effect of degeneration on pressure distribution in axial loading reported by Horst and Brinckmann [14]. However, the latter authors did not measure stress at the outer rim of the endplate. In line with the current study and these finite element model predictions, the location of endplate fractures in compression also was found to be more peripheral in degenerated discs [29]. As far as we know no studies have compared failure location in sustained cyclic versus one-cycle compression. In conclusion, stress distribution over the endplate was found to be fairly uniform. At low compression forces, the stress was the highest centrally. With increased compression and after sustained compression the uniformity increased mainly through an increase of stress in the periphery. No stress peaks were found to occur after sustained loading. The results of this study imply that a non-degenerated disc provides an effective mechanism to distribute stress over the endplate, avoiding the occurrence of stress peaks with increased compression. Even after sustained loading this mechanism is effective in spite of the reduced pressure in the nucleus pulposus. Nevertheless, this mechanism might fall short in two aspects. It might be argued that if the endplate is more vulnerable in the periphery, even the limited increase in peripheral stress might cause damage. However, the trabecular support of the vertebral endplate appears to be only slightly less strong peripherally than centrally [30] and the preferential location for fractures appears to be in the center of the endplate [31,32]. On the other hand, the pressure in the central part of the endplate remained high over a prolonged period. This might cause failure in the central endplate which could actually have been avoided by a stronger unloading of this part of the endplate. Alternative explanations for failure in sustained or repetitive compression, such as creep and fatigue failure [4] would then appear more likely candidates. In addition, the stress as measured in our study probably consists of a component carried by the fluid phase (pore pressure) and a component carried by the solid phase of the material. In sustained loading, a shift of pore pressure to solid stress will occur [33]. Since pore pressure would presumably not lead to damage, whereas solid stresses

could induce failure, this shift might account for damage as well and therefore needs to be quantitatively studied.

Acknowledgements

We would like to thank Mr. W. van de Wijdeven for technical assistance in the data collection, Dr. M. Mullender for reviewing the manuscript and two anonymous reviewers for their constructive criticism.

References

[1] Dieën JHv, Weinans H, Toussaint HM. Fractures of the lumbar vertebral endplate in the etiology of low back pain. A hypothesis on the causative role of spinal compression in a-specific low back pain. Med Hypotheses 1999;53(3):246–52.
[2] Brinckmann P, Biggeman M, Hilweg D. Prediction of the compressive strength of human lumbar vertebrae. Clin Biomech 1989:1–27.
[3] Hansson TH, Roos B, Nachemson A. The bone mineral content and ultimate compressive strength in lumbar vertebrae. Spine 1980;5(Suppl 12):46–55.
[4] Dieën JHv, Toussaint HM. Evaluation of the probability of spinal damage caused by sustained cyclic compression loading. Hum Factors 1997;39(3):469–80.
[5] Brinckmann P, Biggeman M, Hilweg D. Fatigue fracture of human lumbar vertebrae. Clin Biomech 1988;3(Suppl 1):1–27.
[6] Hansson TH, Keller TS, Spengler DM. Mechanical behaviour of the human lumbar spine II. Fatigue strength during dynamic compressive loading. J Orthop Res 1987;5:479–87.
[7] Coventry MB, Ghormley RK, Kernohan JW. The intervertebral disc: its microscopic anatomy and pathology. J Bone Jt Surg 1945; 27(3):460–74.
[8] Vernon-Roberts B, Pirie CJ. Degenerative changes in the intervertebral discs of the lumbar spine and their sequelae. Rheumatol Rehabil 1977;16:13–21.
[9] Vernon–Roberts B, Pirie C. Healing trabecular microfractures in the bodies of lumbar vertebrae. Ann Rheumatol Dis 1973;32:406–12.
[10] Hilton RC, Ball J, Benn RT. Vertebral end-plate lesions (Schmorl's nodes) in the dorsolumbar spine. Ann Rheum Dis 1976;35:127–32.
[11] Hansson T, Roos B. The amount of bone mineral and schmorl nodes in lumbar vertebrae. Spine 1983;8:266–70.
[12] McMillan DW, Garbutt G, Adams MA. Effect of sustained loading on the water content of intervertebral discs: implications for disc metabolism. Ann Rheum Dis 1996;55:1–8.
[13] Adams MA, McMillan DW, Green TP, Dolan P. Sustained loading generates stress concentrations in lumbar intervertebral discs. Spine 1996;21:434–8.
[14] Horst M, Brinckmann P. Measurement of the distribution of axial stress on the end-plate of the vertebral body. Spine 1981;6:217–32.
[15] Ranu HS, Denton RA, King AI. Pressure distribution under an intervertebral disc - an experimental study. J Biomech 1979; 12(10):807–12.
[16] Ranu HS. Measurement of pressures in the nucleus and within the annulus of the human spinal disc: due to extreme loading. Proceedings of the Institution of Mechanical Engineers. Part H – J Eng Med 1990;204(3):141–6.
[17] Ranu HS. Time dependent response of human intervertebral disc to loading. Eng Med 1985;14(1):43–5.
[18] Haut R. Contact pressures in the patellofemoral joint during impact loading on the human flexed knee. J Orthop Res 1989; 7:272–80.
[19] Bass EC, Duncan NA, Hariharan JS, Dusick J, Bueff U, Lotz JC. Frozen storage affects the compressive creep behavior of the porcine intervertebral disc. Spine 1997;22(24):2687–876.
[20] Oshima H, Ishihara H, Urban JP, Tsuji H. The use of coccygeal discs to study intervertebral disc metabolism. J Orthop Res 1993;11(3):332–8.
[21] Chatani K, Kusaka Y, Mifune T, Nishikawa H. Topographic differences of 1H-NMR relaxation times (T1,T2) in the normal intervertebral disc and its relationship to water content. Spine 1993;18(15):2271–5.
[22] Kingma I, Dieën JHv, Nicolay K, Maat JJ, Weinans H. Monitoring water content in deforming intervertebral disc tissue by finite element analysis of MRI data. Magn Res Med 2000;44:650–4.
[23] Burns ML, Kaleps I, Kazarian LE. Analysis of compressive creep behaviour of the intervertebral unit subjected to a uniform axial loading using exact parametric solution equations of Kelvin-solid models- Part I Human intervertebral joints. J Biomech 1984; 17:113–30.
[24] Silva MJ, Keaveny TM, Hayes WC. Load sharing between the shell and centrum in the lumbar vertebral body. Spine 1997;22(2):140–50.
[25] McMillan DW, McNally DS, Garbutt G, Adams MA. Stress distributions inside intervertebral discs: the validity of experimental 'stress profilometry'. Proc Ins Mech Eng 1996;210:81–7.
[26] Holmes AD, Hukins DWL. Response of the end-plate to compression of the spine. Eur Spine J 1993;2:16–21.
[27] Shirazi-Adl A, Shrivastava SC, Ahmed AM. Stress analysis of the lumbar disc-body unit in compression. Spine 1984;9:120–34.
[28] Kurowski P, Kubo A. The relationship of degeneration of the intervertebral disc to mechanical loading conditions on lumbar vertebrae. Spine 1986;11:726–31.
[29] Perey O. Fracture of the vertebral endplate in the human spine. Acta Orthop Scand 1957.
[30] Keller TS, Hansson TH, Abram AC, Spengler DM, Panjabi MM. Regional variations in the compressive properties of lumbar vertebral trabeculae: Effects of disc degeneration. Spine 1989; 14(Suppl 25):1012–9.
[31] Hansson T, Roos B. The relation between bone mineral content, experimental compression fractures and disc degeneration. Spine 1981;6:147–53.
[32] Begg AC. Nuclear herniations of the intervertebral disc. J Bone Jt Surg Br Vol 1954;36B:180–93.
[33] Argoubi M, Shirazi-Adl A. Poroelastic creep response analysis of a lumbar motion segment in compression. J Biomech 1996; 29(10):1331–9.